Effect of crystalline structure on terbuthylazine degradation by H_2O_2-assisted TiO_2 photocatalysis under visible irradiation

Jianjun Tang*, Yiqing Chen, Zijun Dong

Shenzhen Key Laboratory of Industrial Water Conservation and Municipal Wastewater Reclamation Technology, Shenzhen Polytechnic, Guangdong 518055, China

ARTICLE INFO

ABSTRACT

Various methods for shifting the optical response of TiO_2 into the visible (Vis) range have been reported. Herein, we reported the application of a $TiO_2/H_2O_2/Vis$ process and the effects of TiO_2 crystalline structure on the degradation of terbuthylazine. The results indicated that TiO_2 crystalline structure and H_2O_2 addition had significant effects on terbuthylazine degradation: its degradation rate could be increased from 7% to 70% with H_2O_2 addition after 180 min of reaction, the synergistic degradation of terbuthylazine by TiO_2-Fe^{3+} was substantially accelerated, with the degradation rate reaching up to 100% after 20 min of reaction, and rutile TiO_2 showed better photocatalytic activity and a more obvious synergistic effect than anatase TiO_2. The addition of free-radical scavengers (*tert*-butyl alcohol or methanol) inhibited the degradation efficiency of rutile TiO_2, but had a relatively minor effect on anatase TiO_2. Fluorescence spectrophotometry analysis indicated that hydroxyl free radicals could be continuously produced when using rutile TiO_2 as the photocatalyst. Degradation of terbuthylazine catalyzed by rutile TiO_2 occurred mainly in solution, but occurred on the particle surface of the photocatalyst when catalyzed by anatase TiO_2. This study provides new insight into the role of TiO_2 crystalline structure on the degradation of terbuthylazine and its photocatalytic degradation mechanism.

© 2018 The Research Center for Eco-Environmental Sciences, Chinese Academy of Sciences.
Published by Elsevier B.V.

Introduction

Terbuthylazine, a widely used herbicide, has been identified as an endocrine disrupting chemical (EDC) and is recalcitrant toward remediation and toxic to microorganisms (Andrea et al., 2018). Advanced oxidation processes (AOPs) have been previously described as promising methods to remove EDCs from contaminated water when conventional water treatment processes are not efficient enough (Cunff et al., 2018). Among these methods, the TiO_2-based photocatalysis method has attracted the most attention in the past few years because it is relatively cheap, nontoxic, and chemically stable.

It is now commonly accepted that the TiO_2 photocatalyst is first excited by ultraviolet (UV) light and subsequently initiates the photodegradation process (Hoffmann et al., 1995). However, artificial UV light sources tend to be expensive, and the UV light component of sunlight reaching the earth surface that can excite TiO_2 photocatalysis accounts only for a small portion (3%–5%) of the solar spectrum in comparison to the visible (Vis) region (45%) (Li et al., 2007; Subramanian et al., 2004), and this

* Corresponding author. E-mail: tangjj7384@sina.com. (Jianjun Tang).

limitation hinders the practical engineering applications of TiO_2-based photocatalysis.

In order to effectively utilize solar energy, considerable efforts have been devoted to improving the utility of TiO_2 by shifting its optical response from the UV to the visible spectral range, using methods such as transition metal (Lam et al., 2007; Janczyk et al., 2008) and non-metal doping (Sun et al., 2008; Zaleska et al., 2008), dye sensitization (Chatterjee et al., 2006; Ding et al., 2005), and coupling with other narrow-band-gap semiconductors (Sun et al., 2012; Li et al., 2014a). Recently, the use of a combination of H_2O_2 and TiO_2 has been reported for the photocatalytic oxidation of non-dye organic contaminants under visible irradiation, such as linuron (Yao and Chu, 2009, 2010), atrazine (Tang et al., 2010), phenol (Tang et al., 2011), prometryn (Li et al., 2014b) and sodium pentachlorophenate (Liu et al., 2015). The general mechanism of H_2O_2/TiO_2 visible-light-driven photocatalysis was ascribed to the chemisorption of H_2O_2 on the surface of TiO_2 and the subsequent formation of a yellow surface complex, which could be sensitized and excited under visible irradiation (Li et al., 2011; Ohno et al., 2001; Takahara et al., 2005). These studies suggest routes for the utilization of visible light in TiO_2 photocatalytic reactions and the consequent effective utilization of solar light.

Although the interaction between H_2O_2 and TiO_2 is well documented, the degradation mechanism of organic compounds in the H_2O_2/TiO_2/Vis system is still not well understood. Furthermore, current studies indicate that rutile TiO_2 (TIO-R) shows a greater visible-light photocatalytic activity than anatase TiO_2 (TIO-A) in the presence of H_2O_2 (Ohno et al., 2001; Yao and Chu, 2009, 2010; Li et al., 2014a). However, we should recall that rutile TiO_2 is believed to show very poor photocatalytic activity, and to the best of our knowledge, there still remains a lack of understanding of the factors responsible for this difference. It is necessary to deepen the understanding of this photocatalytic reaction mechanism.

In view of these facts, the present study focused on the photocatalytic degradation mechanism of terbuthylazine (a non-dye organic matter) under visible irradiation with H_2O_2 assistance, and the effects of TiO_2 crystalline structure (anatase or rutile) were also studied.

1. Materials and methods

1.1. Photocatalytic experiments

The photodegradation of terbuthylazine was carried out in a batch reactor, in which the TiO_2 (or Fe^{3+}) photocatalyst was mixed with a 80 mL solution of 7 mg/L terbuthylazine ($C_9H_{16}ClN_5$, 99.4% purity). The light source was a 200 W xenon lamp (CMH250, Instruments of Beijing Normal University, China) equipped with a 420 nm cutoff filter. The light

intensity of the Xe lamp reaching the surface of the reactor was 80 W/m^2, and the experimental condition was denoted as Vis (for visible light). Anatase TiO_2 (KY-TiO_2-01, Shanghai Cai Yu Nano Technology Co., Ltd., China) and rutile TiO_2 (KY-TiO_2-03, Shanghai Cai Yu Nano Technology Co., Ltd., China) were used as catalysts and labeled as TIO-A and TIO-R, respectively. Their characteristic parameters, based on the results of X-ray diffraction (XRD) (D/max 2500PCX, Rigaku, Japan) and Brunauer–Emmett–Teller (BET) analysis (Flow Prep 060, Micrometrics, USA), are shown in Table 1. Except when stated otherwise, all the experiments were conducted under fixed conditions according to our previous study (Li et al., 2014b), initial pH 3.3, 1.32 mmol/L of H_2O_2, 1 g/L of TiO_2 photocatalyst, and 34 mg/L of Fe^{3+} ($FeCl_3$).

During the experiment, the aqueous suspensions containing the necessary components were first stirred in the dark for 30 min, and then subjected to visible irradiation for the photocatalytic experiment. At given intervals, samples were collected and filtered (0.45 μm microporous membrane) prior to determining the concentrations.

1.2. Preparation of CO_3^{2-}-saturated photocatalyst

First, 5 g of the photocatalyst (TIO-A or TIO-R) was mixed by stirring in the dark for 24 hr, with 50 mL of a 1 mol/L Na_2CO_3 solution, and then filtered through a 0.45 μm membrane. The resulting solids were freeze-dried at 70°C for 24 hr and stored prior to use (labeled as TIO-A-CO_3 and TIO-R-CO_3, respectively).

1.3. Analytical methods

The concentration of terbuthylazine was determined using a high-performance liquid chromatography (HPLC) system (2695, Waters, USA) equipped with a Symmetry C18 column (5 μm, 4.6 mm × 150 mm) and a photo-diode array (PDA) detector (2998, Waters, USA) with a detection wavelength λ of 224 nm. The samples were separated in the system using an injection volume of 10 μL, a mobile phase (methanol: water 70:30 V/V), and a flow rate of 1.0 mL/min. The concentration of H_2O_2 was determined by the N,N-dimethyl-p-phenylenediamine (DE-PPD)/horseradish peroxidase method (Bader et al., 1988). The total organic carbon (TOC) was measured using a total organic carbon analyzer (TOC-VCPH/CPN, Shimadzu, Japan), the concentration of Cl^- was determined using a ion chromatograph (Isc-1500, Dionex, USA), and degradation intermediates were determined using a liquid chromatography-mass spectrometer (LC-MS) (Lcq Deca XP, Thermo Finnigan, USA). The concentration of hydroxyl (·OH) free radicals was determined using a fluorescence spectrophotometer (F-7000, Hitachi, Japan) with 3.0 mmol/L of phthalic acid (pH 11) as the molecular probe (Ishibashi et al., 2000).

2. Results

2.1. Photocatalytic degradation of H_2O_2 under visible irradiation

The UV–Vis absorption spectra of the samples, treated and untreated with H_2O_2, are shown in Fig. 1. Neither TIO-A nor TIO-R absorbs visible light at wavelengths above 400 nm, but

Table 1 – Characteristics of TiO_2 photocatalysts.			
Sample name	Anatase	Particle size (nm)	Surface area (m^2/g)
TIO-A	>99%	20	65
TIO-R	<1%	35	40
TIO-A: anatase TiO_2; TIO-R: rutile TiO_2.			

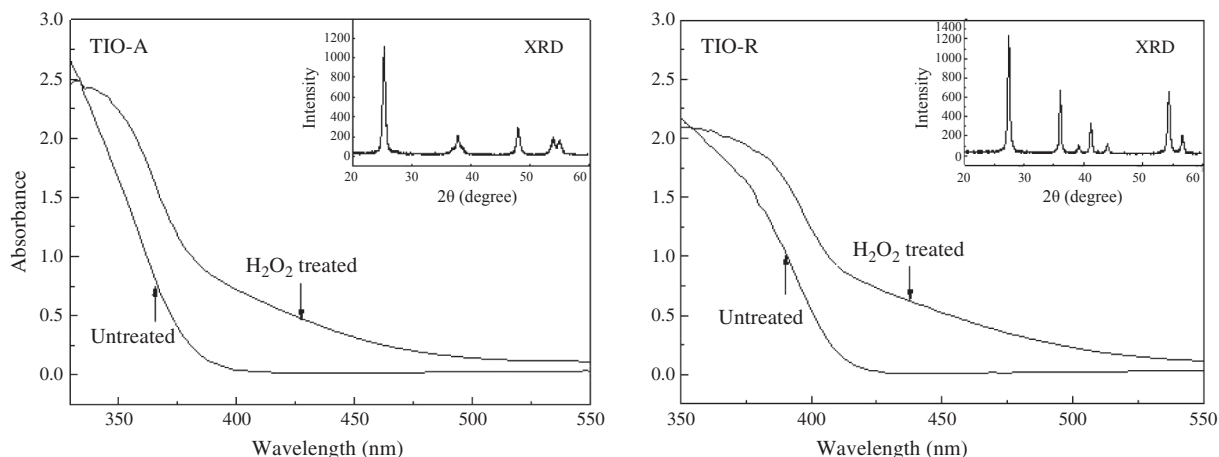**Fig. 1 – Effects of H₂O₂ treatment on the light absorption characteristics of TiO₂. Insets: X-ray diffraction (XRD) of TIO-A and TIO-R.**

the absorption of visible light after treatment with 0.168 mol/L of H_2O_2 was very strong and resulted in a new absorption band in the visible range of 400–500 nm. Moreover, after being immersed into the H_2O_2 solution, both forms of TiO_2 turned pale yellow, which faded gradually following their exposure to natural indoor light. The absorption and color change of TiO_2 resulted from the TiO_2 surface absorption and the formation of a complex due to the interaction between TiO_2 and H_2O_2 (Li et al., 2011; Ohno et al., 2001).

Since H_2O_2 plays a major role in this system, the simultaneous decomposition of H_2O_2 by TiO_2 under visible irradiation was studied using H_2O_2. First of all, the TiO_2 photocatalysts was put into the H_2O_2 solution with an initial concentration of 1.32 mmol/L. The solution was stirred in the dark for 30 min. Then, the solution was under visible light irradiation when keep stirring. Fig. 2 shows that the two TiO_2 photocatalysts exhibit some adsorption capacity toward H_2O_2 during the first 30 min, but TIO-R showed a relatively weaker

adsorption capacity owing to its larger particle size and smaller specific surface area (SSA). The decay of H_2O_2 was noticeably inhibited at pH 3.3 and under visible irradiation, but declined significantly following the addition of TIO-A or TIO-R, indicating that H_2O_2 can be photocatalyzed by TiO_2 under visible irradiation.

Fig. 3 shows that the presence of Vis/H_2O_2 did not have any effect on the degradation of terbuthylazine, and both TIO-A and TIO-R were capable of degrading terbuthylazine. The degradation rate increased from 7% to 70% on the addition of H_2O_2 after 180 min of reaction; TIO-R exhibited a higher catalytic activity than that of TIO-A, which is consistent with the experimental results reported by Yao and Chu (2009, 2010). Both TIO-A and TIO-R had no effect on the degradation of terbuthylazine when their active sites adsorbed CO_3^{2-} to saturation.

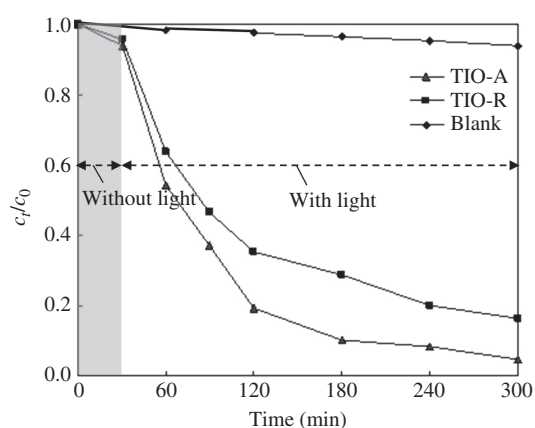Fig. 4 shows the HPLC and LC-MS spectra of terbuthylazine degradation by the TIO-R/H_2O_2/Vis system. The spectra

Fig. 2 – H₂O₂ decomposition by TiO₂ visible-light (Vis) photocatalysis. c_t: different reaction time concentration; c₀: initial concentration.
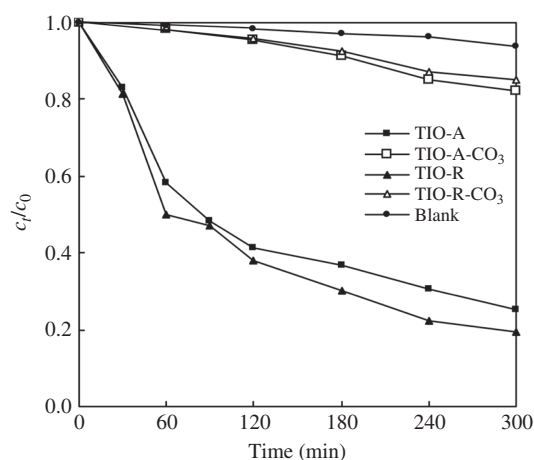

Fig. 3 – Comparison of terbuthylazine photocatalytic degradation under different conditions. TIO-A-CO₃ and TIO-R-CO₃ refer to Section 1.2.
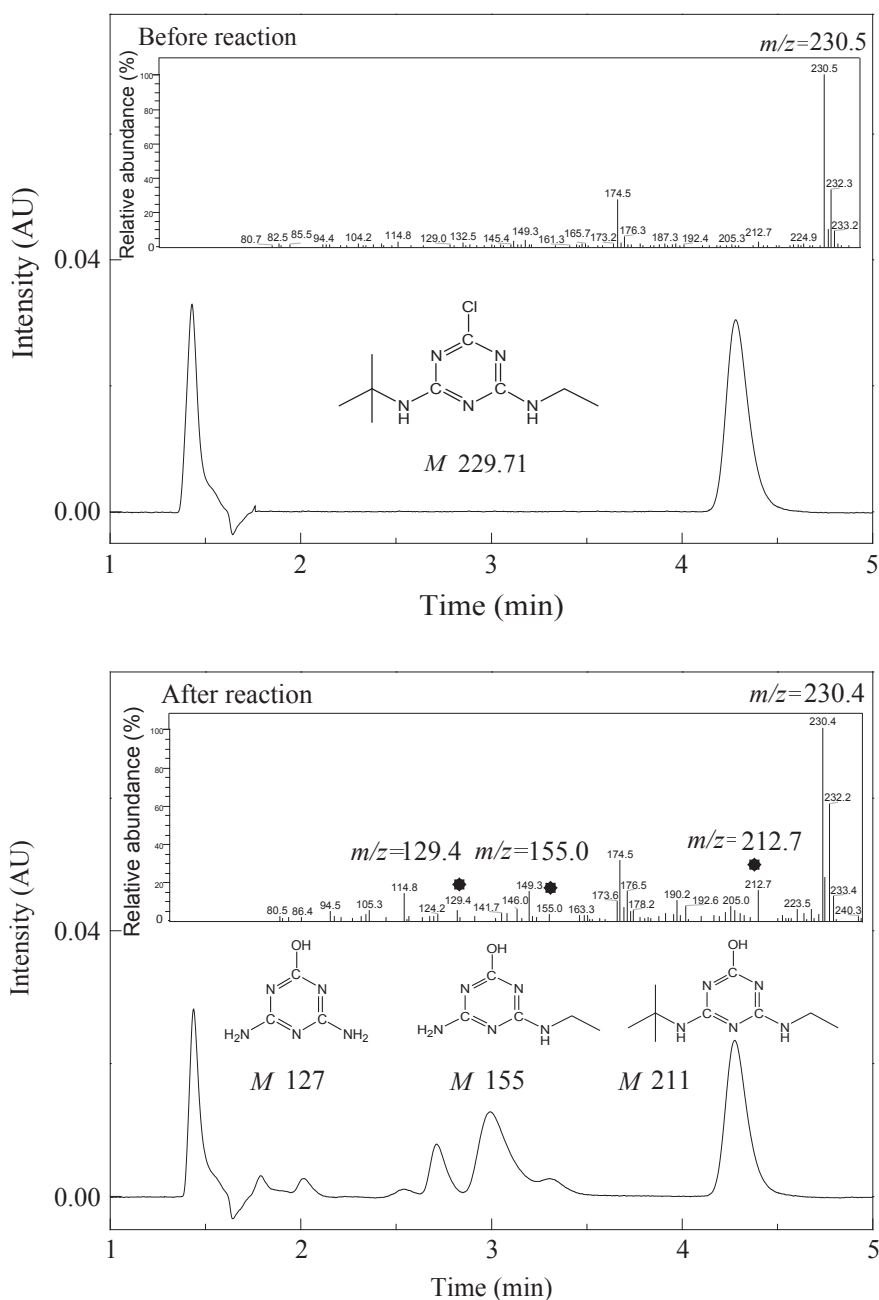
Fig. 4 – LC–MS (Liquid chromatograph-mass spectrometer) spectra of the reaction system before reaction and after 120 min reaction. *m/z*: mass-to-charge ratio; M: mass.

indicated that some degradation intermediates were generated in the terbuthylazine degradation process. The experimental results also indicated that the Cl^- concentration was about 1.0 mg/L after 60 min reaction, and then the Cl^- concentration is stable, which indicated that the degradation of terbuthylazine started with dechlorination and that the dechlorination reaction was complete.

Fig. 5 shows the results of terbuthylazine removal during the degradation process. It can be seen that the reductions in the H_2O_2 and terbuthylazine concentrations were identical. At the initial stage of reaction, the terbuthylazine degradation rate was very fast with rapid H_2O_2 loss.

However, at the later reaction stage, as the H_2O_2 concentration was very low, the terbuthylazine degradation rate was slowed down. The initial concentration of H_2O_2 was 1.32 mmol/L in the reaction system based on the theoretical concentration for the complete mineralization of terbuthylazine. The H_2O_2 was almost depleted after 300 min of reaction, while the degradation rate of terbuthylazine was about 80% and the TOC removal rate was only 20%. This indicated that the reaction system has a low degradation efficiency and H_2O_2 utilization efficiency. In practice, this means that a large excess of H_2O_2 needs to be added to the system to continue the reaction at
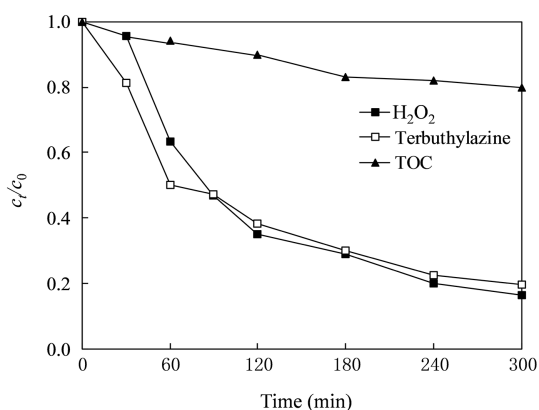
Fig. 5 – Comparison of terbuthylazine degradation rate, total organic carbon (TOC) removal rate and H_2O_2 decomposition rate.
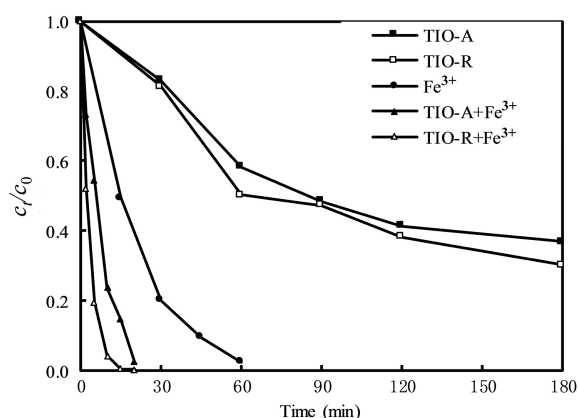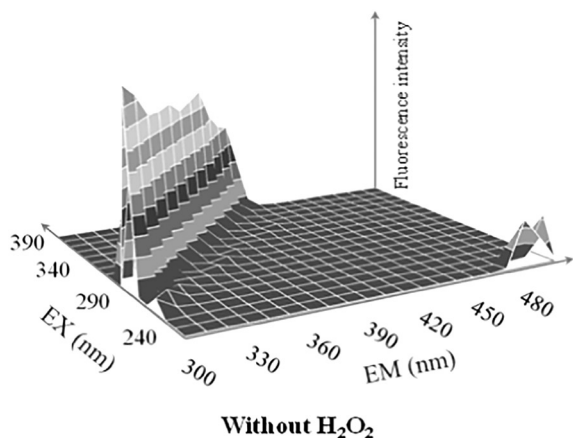

Fig. 6 – Comparison of terbuthylazine degradation rate under different experimental conditions.

high efficiency, as H_2O_2 can be decomposed through many processes such as reduction and oxidation.

In order to improve the H_2O_2 utilization efficiency, we studied the synergistic effect of adding Fe^{3+} into the reaction system. Fig. 6 shows that the Fenton-like reaction system, consisting of 34 mg/L of Fe^{3+} and H_2O_2, helped achieve a degradation rate of almost 100% after 60 min of reaction. Furthermore, the synergistic effect of Fe^{3+} with TIO-A or TIO-R significantly accelerated the degradation of terbuthylazine, reaching up to 100% after 20 min of reaction. Additionally, TIO-R showed a significantly greater synergistic effect than that of TIO-A.

2.2. Analysis of hydroxyl (·OH) free radicals

In order to determine whether ·OH free radicals are involved in the reaction, we investigated the ·OH free-radical production rate based on the intensity of the fluorescence peak at 426 nm with 312 nm excitation. Fig. 7 shows the 3D fluorescence spectra of the reaction system that used TIO-R as the photocatalyst for a reaction time of 30 min. The results show the generation of a pronounced fluorescence peak on adding H_2O_2 at an initial concentration of 1.32 mmol/L, whereas no fluorescence peak was detected without H_2O_2 addition.

·OH free radicals are the main active species in the photocatalytic reaction system, and can react with phthalic acid to generate the fluorescent substance 2,5-dihydroxyterephthalic acid (TA-OH), which emits fluorescence at around 426 nm on excitation of an absorption band at 312 nm (Bader et al., 1988). Hence, the fluorescence peak of the photocatalytic reaction system was attributed to the production of TA-OH by ·OH free radicals and phthalic acid. Fig. 8 further demonstrates that the fluorescence intensity varied with the irradiation period, indicating the continuous generation of ·OH free radicals in the reaction system.

Fig. 9 represents the linear relationship between the concentration of ·OH free radicals and the duration of visible irradiation. ·OH free radicals could be constantly produced in the TIO-R/H_2O_2/Vis reaction system; in contrast, there was no detectable generation in either the TIO-A reaction system or the reaction systems using TIO-A-CO_3 or TIO-R-CO_3 as the photocatalysts.
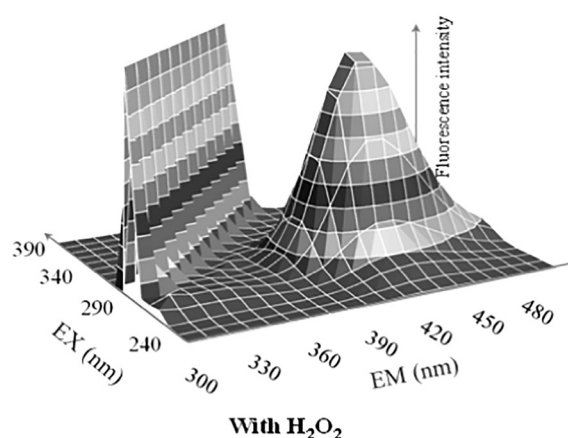

Fig. 7 – Three dimensional fluorescence spectra of the phthalic acid solution system. EX: exciting light; EM: emitted light.
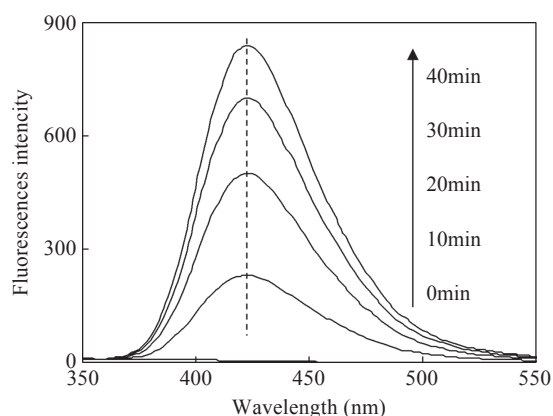
Fig. 8 – Temporal curves of fluorescence intensity in the presence of TIO-R/H_2O_2 under visible light irradiation.
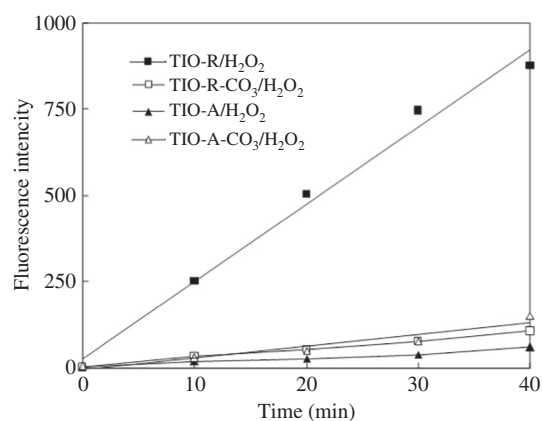

Fig. 9 – Comparison of fluorescence intensities of TIO-A and TIO-R in the presence of Vis/H_2O_2.

2.3. Influence of free-radical inhibitors

Free-radical inhibitors such as methanol and *tert*-butyl alcohol react rapidly with ·OH free radicals in water, thereby interrupting the entire free-radical chain reaction. Therefore, determination of the impacts of free-radical inhibitors and their concentrations can be used to assess whether the reaction is a ·OH reaction mechanism or a solution reaction.

Table 2 shows the impacts of free-radical inhibitors on the H_2O_2-assisted visible-light photocatalytic degradation of

terbuthylazine catalyzed by TIO-A and TIO-R for a reaction time of 180 min. The results show that the addition of methanol or *tert*-butyl alcohol into the TIO-R photocatalytic reaction system significantly reduced the degradation rate of terbuthylazine based on the inhibitor concentration. On the contrary, the addition of methanol or *tert*-butyl alcohol into the TIO-A photocatalytic reaction system did not have a significant effect on the degradation rate of terbuthylazine.

3. Discussion

The absorption spectra of TiO_2 and H_2O_2 are limited to the UV region with a wavelength range of below 400 nm, but H_2O_2 can adsorb onto the particle surface of TiO_2 to form complexes such as on-top, μ-peroxide, and η^2-peroxide, which extend the absorption wavelength of TiO_2 to the visible range (Ohno et al., 2001; Takahara et al., 2005). The on-top and μ-peroxide complexes are present on the particle surface of both TIO-A and TIO-R, but η^2-peroxide is present only on the particle surface of TIO-R.

By taking into account the adsorption structure and experimental results obtained in this study, the increase in the amount of the ·OH free radicals for TIO-R can be explained based on the contribution of the H_2O_2 adsorption structure η^2-peroxide. On-top and μ-peroxide are excited by visible light to generate a surface-active species, which are adsorbed ·OH radicals, which cannot react with the molecular probe (phthalic acid) to produce a fluorescent substance (TA-OH). Conversely, η^2-peroxide is a unique epoxy structure that can be excited by visible light to generate ·OH free radicals (Hirakawa and Nosaka, 2002; Hirakawa et al., 2007); the generated ·OH free radicals react with the molecular probe to generate a fluorescent substance (TA-OH) that can be measured via fluorescence spectrophotometry. Thus, the radicals in the TIO-A/H_2O_2/Vis system cannot be detected via fluorescence spectrophotometry but still exert a certain degradation effect on terbuthylazine, as shown in Fig. 3. H_2O_2 and CO_3^{2-} share common adsorption sites on the particle surface of TiO_2, although CO_3^{2-} has a greater adsorption capacity. Therefore, the saturation of adsorption sites on the surface of TIO-A or TIO-R by CO_3^{2-} impedes the adsorption of H_2O_2 onto the particle surface of TiO_2 and thus the formation of complexes.

Adsorbed ·OH radicals are the main active species in the TIO-A/Vis/H_2O_2 reaction system, and therefore, the degradation of terbuthylazine predominantly occurred on the particle surface of TIO-A photocatalysts. However, free-radical inhibitors such as *tert*-butyl alcohol and methanol only affect the degradation of terbuthylazine via competitive adsorption and oxidation on the particle surface of photocatalysts, and

Table 2 – Effects of *tert*-butyl alcohol and methanol on TIO-A and TIO-R photocatalytic degradation of terbuthylazine in the presence of Vis/H_2O_2.

	TIO-A				TIO-R		
Tert-butanol concentration (mg/L)	Degradation rate	Methanol concentration (mg/L)	Degradation rate	*Tert*-butanol concentration (mg/L)	Degradation rate	Methanol concentration (mg/L)	Degradation rate
0	63.2%	0	63.2%	0	69.9%	0	69.9%
5	59.9%	4	61.5%	5	50.6%	4	48.5%
50	56.3%	40	58.6%	50	34.3%	40	35.6%
250	51.8%	200	54.8%	250	15.7%	200	14.3%

hence, these inhibitors exert a relatively small effect on the degradation rate. However, the degradation photocatalyzed by TIO-R mainly occurred in solution, involving ·OH free radicals in the system. Free-radical inhibitors react with the resulting ·OH free radicals, thereby interrupting the entire free-radical chain reaction and significantly reducing the degradation rate of terbuthylazine.

The significant synergistic acceleration of degradation by Fe^{3+} with TIO-A or TIO-R can be justified as follows: H_2O_2 adsorbs onto the particle surface of TIO-A or TIO-R to form complexes that trigger a primary reaction after being excited by visible light to generate reductive intermediates (such as the benzene ring structure) as shown in Fig. 4. The reductive intermediates react with Fe^{3+} to form complexes, and the reductive effect of Fe^{3+} is the main route for Fe^{2+} regeneration that promotes the Fe^{3+}/Fe^{2+} cycle (Du et al., 2006; Jiang et al., 2010), resulting in multi-channel reaction pathways that improve the reaction rate and H_2O_2 utilization efficiency. TIO-R significantly outperforms TIO-A with respect to synergistic effects because of the different degradation pathways between them: the reaction pathway of terbuthylazine degradation catalyzed by TIO-R mainly occurs in solution, which generates more intermediates during the reaction (Tang et al., 2011).

4. Conclusions

(1) Degradation of terbuthylazine in a TiO_2 suspension under visible irradiation occurs only in the presence of H_2O_2, its degradation rate increases from 7% to 70% on adding H_2O_2 after 180 min of reaction, and rutile TiO_2 shows better activity than anatase TiO_2.

(2) TiO_2-Fe^{3+} exhibits a significant synergistic effect on terbuthylazine degradation, with a degradation rate of up to 100% after 20 min of reaction. Moreover, rutile TiO_2 shows a more prominent synergistic effect, but free-radical inhibitors significantly reduce its degradation efficiency, while having a relatively little effect on anatase TiO_2.

(3) Rutile and anatase TiO_2 exhibit different abilities for ·OH free-radical formation, and the degradation of terbuthylazine photocatalyzed by rutile TiO_2 mainly occurs in solution, while it occurs mainly on the particle surface of the catalyst when anatase TiO_2 is used as the photocatalyst.

REFERENCES

Andrea, L.T., Monica, P., Ashleigh, F., 2018. Terbuthylazine and desethylterbuthylazine: Recent occurrence, mobility and removal techniques. Chemosphere 202, 94–104.

Bader, H., Sturzenegge,R, V., Hoigne, J., 1988. Photometric method for the determination of low concentrations of hydrogen peroxide by the peroxidase catalyzed oxidation of N,N-diethyl-p-phenylenediamine (DPD). Wat. Res. 22, 1109–1115.

Chatterjee, D., Dasgupta, S., Rao, N.N., 2006. Visible light assisted photodegradation of halocarbons on the dye modified TiO_2 surface using visible light. Sol. Energy Mater. Sol. Cells 90, 1013–1019.

Cunff, J.L., Tomasic, V., Gomzi, Z., 2018. Photocatalytic degradation of terbuthylazine: Modelling of a batch recirculating device. J. Photochem. Photobiol. A 353, 159–170.

Ding, H., Sun, H., Shan, Y., 2005. Preparation and characterization of mesoporous SBA-15 supported dye-sensitized TiO_2 photocatalyst. J. Photochem. Photobiol. A 169, 101–107.

Du, Y.X., Zhou, M.H., Lei, L.C., 2006. Role of the intermediates in the degradation of phenolic compounds by Fenton-like process. J. Hazard. Mater. 136, 859–862.

Hirakawa, T., Nosaka, Y., 2002. Properties of O_2· and ·OH formed in TiO_2 aqueous suspensions by photocatalytic reaction and influence of H_2O_2 and some ions. Langmuir 18, 3247–3254.

Hirakawa, T., Yawata, K., Nosaka, Y., 2007. Photocatalytic reactivity for O_2^- and OH· radical formation in anatase and rutile TiO_2 suspension as the effect of H_2O_2 addition. Appl. Catal. A Gen. 325, 105–111.

Hoffmann, M.R., Martin, S.T., Choi, W., Bahnemann, D.W., 1995. Environmental applications of semiconductor photocatalysis. Chem. Rev. 95, 69–96.

Ishibashi, K., Fujishima, A., Watanabe, T., 2000. Detection of active oxidative species in TiO_2 photocatalysisusing the fluorescence technique. Electrochem. Commun. 2, 207–210.

Janczyk, A., Wolnicka-Gtubisz, A., Urbanska, K., Kisch, H., Stochel, G., Macyk, W., 2008. Photodynamic activity of platinum(IV) chloride surface-modified TiO_2 irradiated with visible light. Free Radic. Biol. Med. 44, 1120–1130.

Jiang, C.C., Pang, S.Y., Ma, J., 2010. A new insight into Fenton and Fenton-like processes for water treatment. J. Hazard. Mater. 174, 813–816.

Lam, R.C.W., Leung, M.K.H., Leung, D.Y.C., Vrijmoed, L.L.P., Yam, W.C., Ng, S.G., 2007. Visible-light-assisted photocatalytic degradation of gaseous formaldehyde parallel-plate reactor coated with Cr ion-implanted TiO_2 thin film. Sol. Energy Mater. Sol. Cells 91, 54–61.

Li, H.X., Bian, Z.F., Zhu, J., Huo, Y.N., Li, H., Lu, Y.F., 2007. Mesoporous Au/TiO_2 nanocomposites with enhanced photocatalytic activity. J. Am. Chem. Soc. 129, 4538–4539.

Li, X.Z., Chen, C.C., Zhao, J.C., 2011. Mechanism of photodecomposition of H_2O_2 on TiO_2 surfaces under visible light irradiation. Langmuir 17, 4118–4122.

Li, X., Xia, T., Xu, C.H., Murowchick, J., Chen, X.B., 2014a. Synthesis and photoactivity of nanostructured CdS-TiO_2 composite catalyst. Catal. Today 225, 64–73.

Li, Q.K., Zhou, B.Y., Tang, J.J., Chen, Y.Q., 2014b. Degradation of prometryn by TiO_2 visible photocatalysis with H_2O_2 assistance. J. Zhengzhou Univ. (Engineering Science) 35, 55–59.

Liu, W., Liu, H.C., Ai, Z.H., 2015. In-situ generated H_2O_2 induced efficient visible light photo-electrochemical catalytic oxidation of PCP-Na with TiO_2. J. Hazard. Mater. 288, 97–103.

Ohno, T., Masaki, Y., Hirayama, S., Matsumura, M., 2001. TiO_2-photocatalyzed epoxidation of 1-decene by H_2O_2 under visible light. J. Catal. 204, 163–168.

Subramanian, V., Wolf, E.E., Kamat, P.V., 2004. Catalysis with TiO_2/gold nanocomposites. Effect of metal particle size on the fermi level equilibration. J. Am. Chem. Soc. 126, 4943–4950.

Sun, J.H., Qiao, L.P., Sun, S.P., Wang, G.L., 2008. Photocatalytic degradation of organge G on nitrogen-doped TiO_2 catalysts under visible light and sunlight irradiation. J. Hazard. Mater. 155, 312–319.

Sun, Q., Leng, W., Xu, Y., 2012. Effect of surface Fe_2O_3 clusters on the photocatalytic activity of TiO_2 for phenol degradation in water. J. Hazard. Mater. 229, 224–232.

Takahara, Y.K., Hanada, Y., Ohno, T., Ushiroda, S., Ikeda, S., Matsumura, M., 2005. Photooxidation of organic compounds in a solution containing hydrogen peroxide and TiO_2 particles under visible light. J. Appl. Electrochem. 35, 793–797.

Tang, J.J., Liu, S.J., Zou, Y., Xie, W.P., Liu, F.L., 2010. Degradation of atrazine by H_2O_2photocatalyzed under visible irradiation of r-TiO_2. Min. Metall. Eng. 30, 106–109.

Tang, J.J., Fan, X.J., Liu, S.J., Zou, Y., Zhou, K.G., 2011. Degradation of organic pollutants with H_2O_2 photocatalyzed by TiO_2 under visible irradiation. Chin. J. Nonferrous Met. 21, 2017–2022.

Yao, Y.F., Chu, W., 2009. Reaction mechanism of linuron degradation in TiO_2 suspension under visible light irradiation with the assistance of H_2O_2. Environ. Sci. Technol. 43, 6183–6189.

Yao, Y.F., Chu, W., 2010. Linuron decomposition in aqueous semiconductor suspension under visible light irradiation with and without H_2O_2. Chem. Eng. J. 158, 181–187.

Zaleska, A., Sobczak, J.W., Grabowska, E., Hupka, J., 2008. Preparation and photocatalytic activity of boron-modified TiO_2 under UV and visible light. Appl. Catal. B Environ. 78, 92–100.